

*Short Communication*

# Investigation of Electrochemical Migration of Tin and Tin-Based Lead-Free Solder Alloys under Chloride-Containing Thin Electrolyte Layers

Shuyi Jiang<sup>1</sup>, Bokai Liao<sup>2,\*</sup>, Zhenyu Chen<sup>2</sup>, Xingpeng Guo<sup>2</sup>

<sup>1</sup> School of Industrial Design, Hubei University of Technology, Wuhan 430068, China

<sup>2</sup> Hubei Key Laboratory of Materials Chemistry and Service Failure, School of Chemistry and Chemical Engineering, Huazhong University of Science and Technology, Wuhan 430074, China

\*E-mail: [bokailiao@yeah.net](mailto:bokailiao@yeah.net)

*Received:* 13 June 2018 / *Accepted:* 15 July 2018 / *Published:* 1 September 2018

---

The electrochemical migration behaviors of pure tin and tin-based lead-free solder alloys under thin electrolyte layers containing chloride ions were investigated. Impacts of the applied bias voltage and thickness of electrolyte layer on the electrochemical migration processes were studied in detail. Results showed that the mean time to failure first increased and then decreased with increasing electrolyte-layer thickness. The maximum value of failure time was presented at a 200- $\mu\text{m}$ -thickness. The higher bias voltage was applied, the faster rate of dendrite growth was. The migration element of tin-based lead-free solder alloys was tin and the formed dendrites displayed tree- and feather-like structures. Mechanisms relevant have been proposed to explain the electrochemical migration behaviors of tin and tin based solder alloys.

---

**Keywords:** Solder alloy; Corrosion; Electrochemical migration; dendrite

## 1. INTRODUCTION

Electrochemical migration (ECM), a common form of corrosion encountered in the electronics industry [1-3], is generally defined as the transport of metal ions via the continuous adsorbed electrolyte layer between two closely spaced and oppositely biased adjacent conductor lines/traces [4, 5]. The ECM phenomenon includes three essential processes: dissolution of metal, transportation of metal ions and electro-deposition of metal ions [6, 7]. The growth of metallic dendrites during ECM processes may cause insulation-resistance degradation or short circuiting of electronic components. With the trend of

integration to a higher density of electronic components and explosive usage in harsh service scenarios, ECM failure has been reported as a great threat to the reliability of electronics [8-12].

Owing to the inherent toxicity of lead (Pb), lead-bearing solder alloys have been internationally forbidden in the industry of electric appliances[13]. Nowadays, various kinds of tin based lead-free solder alloys have been developed as Pb replacements in the electronics industry, including Sn-Ag, Sn-Cu, Sn-Bi, Sn-Zn, etc. [14, 15]. A large number of studies on ECM behavior of tin-based solder alloys in solutions have been carried out. For example, Medgyes et al. [16] analyzed the effect of sulfate ion concentration on the ECM behavior of SAC305 solder alloy in a Na<sub>2</sub>SO<sub>4</sub> environment using water-drop tests. Yu et al. [17] studied the ECM of Sn-Pb and some lead free solder alloys under distilled water droplets. Minzari et al. [1] investigated the effects of environmental factors on the ECM behavior of Sn, including applied bias voltage, distance between the two electrodes, various contaminants, etc. He further analyzed the dendrite growth mechanism. However, considering the actual service scenarios of electronic devices, ECM of solder alloys is more likely to occur under a thin electrolyte layer on a metal surface produced either by a condensation process under high-humidity conditions or rain & snow [18-20]. Additionally, the chloride ion is considered as one of the most common contaminants for electronic devices, which can originate from human sweat, dust in the air and flux residues used in the soldering process. Furthermore, it has been reported that chloride ions can significantly affect the ECM process [9, 21]. Few reports on the ECM behavior of solder alloys under thin electrolyte layers (TELs) containing chloride ions are available.

In this work, the ECM behavior of tin and tin based lead-free solder alloys in chloride-containing environments was investigated using a TEL method. Compared with the traditional thermal humidity bias (THB) test and water drop (WD) test, the TEL test can guarantee a good reproducibility in test results and *in situ* optical inspection [22]. And the effects of electrolyte layer thickness and bias voltage on ECM behavior are discussed in detail.

## 2. EXPERIMENTAL

### 2.1 Materials and solution preparation

Samples with dimensions 2 mm × 5 mm × 15 mm used in this research were processed from commercial tin and tin based solder alloys, including Sn-3.0Ag, Sn-0.7Cu, Sn-3.0Ag-0.5Cu, Sn-0.3Ag-0.7Cu, Sn-58Bi and Sn-5Sb. Two identical samples were sealed in a cylindrical plastic tube using epoxy resin with gap size of 0.5 mm in parallel direction, one electrode was working electrode and the other was auxiliary electrode. A copper wire was welded on the back of each electrode to guarantee electric conductance during electrochemical tests. All test surfaces were mechanical grinded with 1200 # grit silicon carbide papers. The surfaces were then rinsed with deionized water, degreased with acetone, and dried in cool air. Sodium chloride (NaCl) solution was prepared from analytically pure reagent and deionized water.

## 2.2 Measurement of TEL thickness and ECM test

Electrolyte was added to the surface of electrode to form a thin electrolyte layer. The thickness of the electrolyte layer was measured using a setup consisting of a one-dimension mobile platform, platinum wire (diameter = 0.2 mm), a micrometer and an ohmmeter. Platinum wire was fixed at tail end of mobile platform and micrometer was fixed on mobile platform for measurement of travel distances of the platform and platinum wire. Platinum wire could move along the vertical direction by rotating the micrometer. Ohmmeter was used to measure current value between electrode and platinum wire loop. During measuring process of electrolyte layer thickness, micrometer was rotated to make platinum wire approach electrode surface. Before platinum wire contacted electrolyte layer surface, open-circuit status existed between electrode and platinum wire, and current value was not monitored on the ohmmeter. When platinum wire contacted electrolyte layer surface, current value could be observed on the ohmmeter, and when platinum wire further contacted electrode surface, current value increased instantly. Travel distance of platinum wire was recorded through reading on the micrometer. Difference value of distances of platinum wire contacting electrolyte layer and electrode surface was namely thickness of electrolyte layer. Thickness precision of electrolyte layer tested by the device was consistent with testing precision of micrometer, being 10  $\mu\text{m}$ . The TEL measurement was performed using the method described in our previous work [23-26]. To maintain the stability of the TEL thickness, the electrochemical cell was put into a closed container prior to the ECM test. And aqueous glycerin solution was used to maintain constant 98% relative humidity at a room temperature. The constant direct current bias voltage was applied between the electrodes using a potentiostat and the leakage current was simultaneously recorded by a galvanometer, as shown in Fig.1. All ECM measurements were repeated at least three times to check the reproducibility.

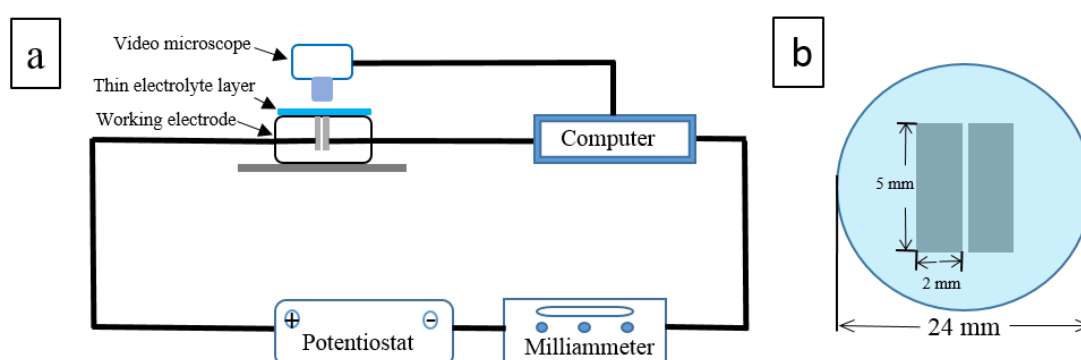


**Figure 1.** (a) Schematic of setups for ECM test under a thin electrolyte layer; (b). Plan form of the working electrode.

## 2.3 Surface characterization

After ECM tests, the samples were dried under a nitrogen gas flow at a room temperature. Morphologies of dendrites generated after ECM tests were examined *ex situ* with a scanning electron microscope (SEM, Phillips Quanta 200) coupled with an energy dispersive spectrometer (EDS).

### 3. RESULTS AND DISCUSSION

#### 3.1. Mean time to failure for ECM tests under TELs at different bias voltages

The current density transients measured between the two electrodes when a bias voltage was applied between them, showed that the abrupt increase of current density was due to the short circuit occurring when dendrites joined the two electrodes [27-29]. The time to failure can be defined as time required for the first dendrite to connect the cathode and anode. Fig. 2 shows the mean time to short circuit for various kinds of solder alloys under 200- $\mu\text{m}$ -thick electrolyte layers containing 1 mM NaCl at different bias voltages. The mean time to failure decreased with the increasing bias voltage. For example, mean time to failure for tin at 3 V is 59 s while it is 0.86 s at a bias voltage of 10 V; the mean time to failure for Sn-0.3Ag-0.7Cu alloy is 76 s at 3 V while it is 1.53 s at 10 V. As the driving force of the ECM process, the increase of applied bias voltage promotes the anodic dissolution rate, migration rate of metal ions and metal ion electro-deposition at the cathode [30, 31]. It is believed that the dendrite growth rate increases with the increasing bias voltage, which is in accordance with the results obtained by Lee [32]. Moreover, under the same bias voltage, tin -based alloys display longer failure time than that of tin, indicating that the addition of alloy elements can suppress the ECM process.

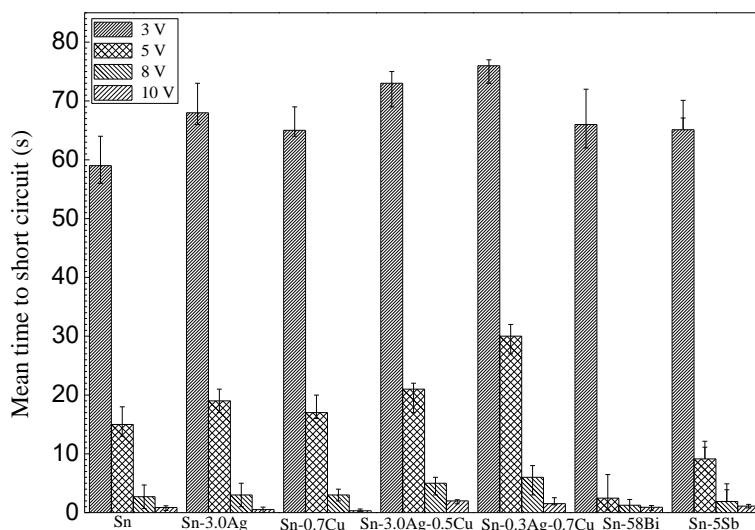
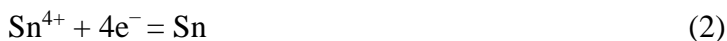


**Figure 2.** Mean time to failure for the ECM of different lead-free solder alloys in 200- $\mu\text{m}$ -thick electrolyte layers containing 1 mM Cl<sup>-</sup> at various bias voltages.

#### 3.2. Mean time to failure for ECM processes under TELs with various thicknesses

Figure 3 shows the mean time to failure for various kinds of solder alloys under TELs containing 1 mM NaCl of various thicknesses with a bias voltage of 3 V. It can be found that the mean time to short circuit first increases and then decreases with increasing electrolyte-layer thickness. For example, the maximum value is obtained under a 200- $\mu\text{m}$ -thick electrolyte layer. The shorter failure time

indicates a faster dendrite growth rate [33], and the dendrite growth under a thin electrolyte layer containing chloride ions can be mainly attributed to the reductions of local Sn<sup>4+</sup> and/or Sn<sup>2+</sup>, according to the following reactions (1) and (2) [1, 21].



The concentration of Sn<sup>4+</sup>/Sn<sup>2+</sup> is decided by the amount of ions and the electrolyte volume as given by Eq. (3). According to our previous work [24], as for the ECM process occurring under TEL conditions, it has been proved that the local concentration of metal ions first decreased and then increased with increasing electrolyte-layer thickness. Thus, the failure time first increased and then decreased with the increase of electrolyte-layer thickness.

$$C_{\text{Sn}^{2+}/\text{Sn}^{4+}} = \frac{n_{\text{Sn}^{2+}/\text{Sn}^{4+}}}{V} \tag{3}$$

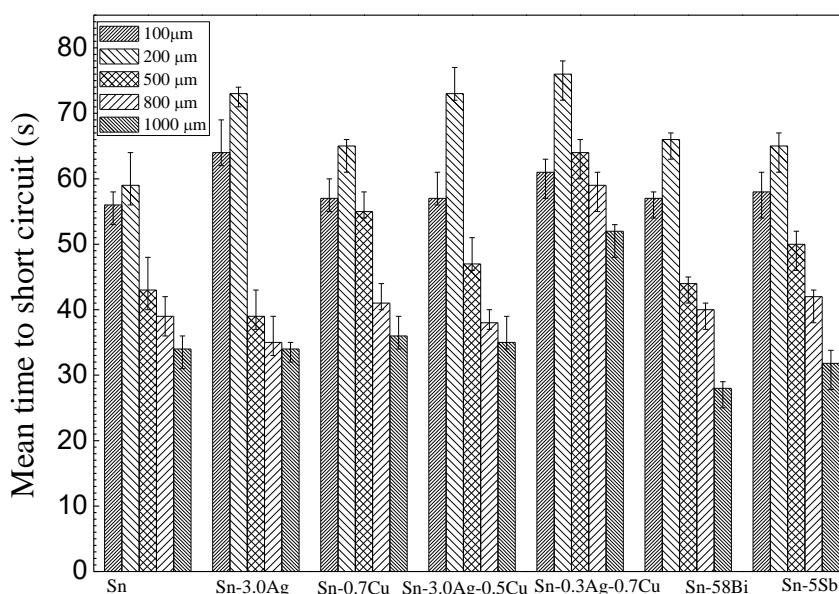


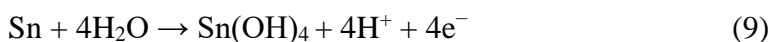
**Figure 3.** Mean time to failure for the ECM of different lead-free solder alloys in electrolyte layers of various thicknesses containing 1 mM Cl<sup>-</sup> at 3 V bias voltage.

### 3.3. Compositions and microstructures of dendrites

The microstructures and compositions of dendrites generated after ECM tests for tin and different tin-based solder alloys are shown in Fig.4. For Sn-3.0Ag, Sn-58Bi and Sn-Ag-Cu series solder alloys, morphologies of the dendrites are similar, maintaining a tree- or needle-like microstructure. One straight trunk has small branches in the vertical direction, and the small branches have the same shape of the entire dendrite. For Sn-0.7Cu and Sn-5Sb solder alloys (Figs.4c and 4g), dendrite displayed a feather-like structure and the longer branches become coarse and denser. Moreover, the dendrites are covered with white precipitates in all cases.

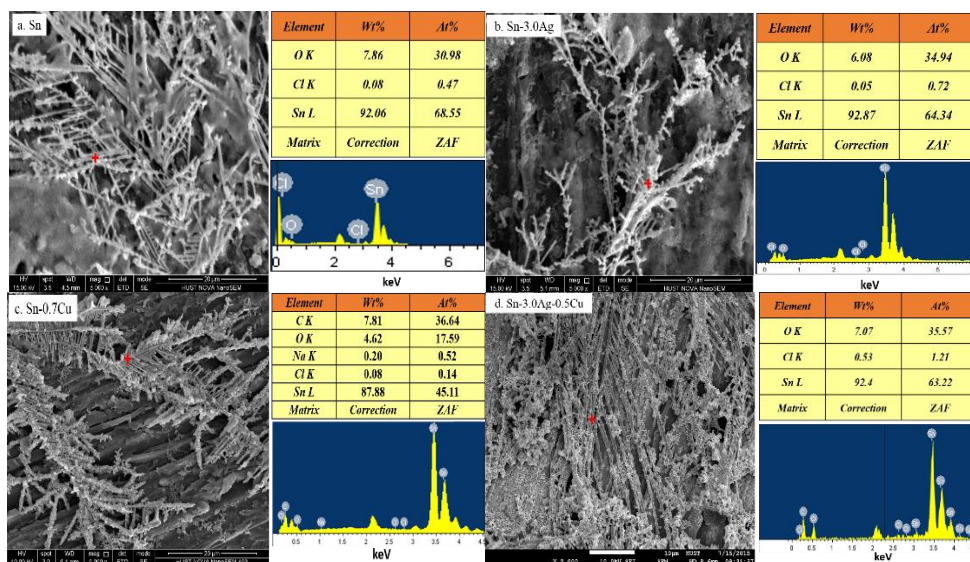
The compositions of dendrites were analyzed using EDS. The corresponding EDS results showed high contents of tin for dendrites obtained for all test solder alloys. For example, dendrites formed for

Sn-3.0Ag alloy consisted of tin (92.87 wt. %), oxygen (6.08 wt. %), and chloride (0.05 wt. %), illustrating that these dendrites were mainly composed of tin. Possible reactions for dendrite growth are as follows [6, 34-36]:



The dissolution of tin [Reaction (4)] and oxidation of water [Reaction (5)] should be the dominant anodic reactions, while the main cathodic reaction is the reduction of H<sub>2</sub>O [Reaction (6)] and dissolved oxygen [Reaction (7)], in which a large amount of OH<sup>-</sup> will be produced at the cathode during ECM. During the ECM process, tin ions from the anode react with OH<sup>-</sup> from the cathode to form precipitates [Reaction (8)]. The direct oxidation of tin to Sn(OH)<sub>4</sub> could occur at the anode side [Reaction (9)] [1]. The tin hydroxide compounds have an amphiprotic property and Sn(OH)<sub>4</sub> will dissolve to form [Sn(OH)<sub>6</sub>]<sup>2-</sup> under basic conditions [Reaction (10)]. Owing to the narrow gap (500 μm) between the two electrodes, [Sn(OH)<sub>6</sub>]<sup>2-</sup> will be transferred to the cathode by the diffusion and conversion effect induced by the hydrogen evolution, and it will be reduced to metallic tin according to the Reaction (11) [1]. And direct reductions of Sn<sup>4+</sup> and Sn<sup>2+</sup> can also boost the dendrite growth [1, 21].

The addition alloy elements, such as Cu, Ag, etc. are also susceptible to ECM [28]. However, due to the formation of intermetallic compounds in these solder alloys, such as Ag<sub>3</sub>Sn and Cu<sub>6</sub>Sn<sub>5</sub>, it is difficult for the alloy elements to escape from the intermetallic compounds [17] and the ECM of alloy elements is inhibited.



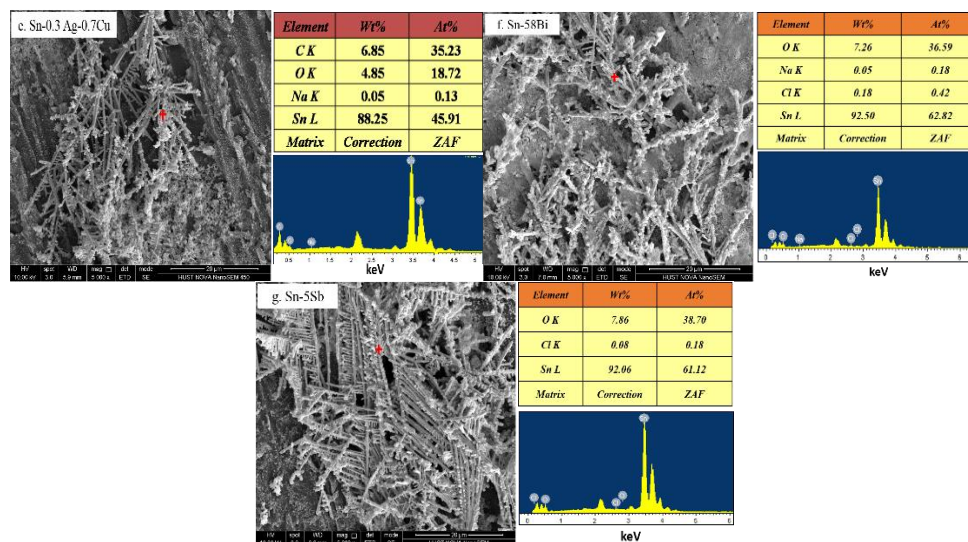


**Figure 4.** Microstructure of dendrites formed after ECM for tin and different tin based solder alloys in 200- $\mu\text{m}$ -thick electrolyte layers containing 1 mM  $\text{Cl}^-$  at 3 V bias voltage: (a) Sn; (b) Sn-3.0Ag; (c) Sn-0.7Cu; (d) Sn-3.0Ag-0.5Cu; (e) Sn-0.3Ag-0.7Cu; (f) Sn-58Bi; (g) Sn-5Sb.

#### 4. CONCLUSION

Electrochemical migration tests on tin and several kinds of lead-free tin based solder alloys under thin electrolyte layers containing chloride ions were investigated using a TEL method. For the selected tin-based solder alloys, the migration element is tin and the obtained dendrites are tree- and/or feather-like structures. As the applied bias voltage increased, the mean time to failure decreased. Moreover, the failure time first increased and then decreased with increasing electrolyte-layer thickness. Moreover, the addition of alloy elements can suppress the ECM phenomenon.

#### ACKNOWLEDGMENTS

The authors thanks the National Natural Science Foundation of China (Nos. 51571098) for their financial support and the Analysis Support of the Analytical and Testing Center, Huazhong University of Science and Technology.

#### References

1. D. Minzari, M.S. Jellesen, P. Møller and R. Ambat, *Corros. Sci.*, 53 (2011) 3366.
2. S. B. Lee, Y. R. Yoo, J. Y. Jung, Y. B. Park, Y. S. Kim, Y. C. Joo, *Thin Solid Films*, 504 (2006) 294.
3. J. W. Yoon, B. I. Noh and S. B. Jung, *Microelectron. Reliab.*, 54 (2014) 410.
4. K. S. Kim, S. B. Jung and D. U. Kim, *J. Mater. Sci-Mater. El.*, 27 (2016) 9676.
5. B. Medgyes, B. Horváth, B. Illés, T. Shinohara, A. Tahara, G. Harsányi and O. Krammer, *Corros. Sci.*, 92 (2015) 43.
6. X. Zhong, L. Chen, B. Medgyes, Z. Zhang, S. Gao and L. Jakab, *RSC Adv.*, 7 (2017) 28186.
7. X. Zhong, L. Chen, J. Hu, Y. Shi, Z. Zhang, D. Zeng and T. Shi, *J. Electrochem. Soc.*, 164 (2017) D342.
8. P. Yi, K. Xiao, C. Dong, S. Zou and X. Li, *Bioelectrochemistry*, 119 (2018) 203.

9. P. Yi, C. Dong, K. Xiao and X. Li, *Appl. Surf. Sci.*, 399 (2017) 608.
10. P. Yi, K. Xiao, K. Ding, C. Dong and X. Li, *Mater. Res. Bull.*, 91 (2017) 179.
11. B. Medgyes, X. Zhong and G. Harsányi, *J. Mater. Sci-Mater. El.*, 26 (2015) 2010.
12. J.Y. Jung, S.B. Lee, Y. C. Joo, H.Y. Lee, Y. B. Park, *Microelectron. Eng*, 85 (2008) 1597.
13. J. Y. Jung, Shin-Bok, Ho Young Lee, Young Chang Joo and Young Bae Park, *J. Electron. Mater.*, 37 (2008) 1111.
14. B. L. Silva, M. G. Xavier, A. Garcia and J. E Spinelli, *Mat. Sci. Eng A-Struct*, 705 (2017) 325.
15. M. Islam, YC Chan, A. Sharif and M. J Rizvi, *J. Alloy. Compd.*, 396 (2005) 217.
16. B. Medgyes, R. Kiss, S. Szurdán, D. Rigler, L. Gál, R. Berényi and G S.Harsányi, *Electrochemical migration investigations on Sn-Sb solder alloys using 3.5 wt.% NaCl solution. 40th International Spring Seminar on Electronics Technology (ISSE), Sofia, Bulgaria, 2017, 1-4.*
17. D.Q. Yu, W. Jillek and E. Schmitt, *J. Mater. Sci-Mater. El.*, 17 (2006) 219.
18. J. C. Liu, Sungwon Park, Nagao Shijo, Masaya Nogi, Hirotaka Koga, Ju Sheng Ma, Gong Zhang and Katsuki Suganuma, *Corros. Sci.*, 92 (2015) 263.
19. F.R.S. U. R. EVANS, *Nature*, 206 (1965) 980.
20. B. Medgyes, L. Gál and D. Szivós, *The effect of NaCl on water condensation and electrochemical migration, IEEE 20th International Symposium for Design and Technology in Electronic Packaging (SIITME), Istanbul, Turkey, 2014, 259-260.*
21. X. Zhong, Guoan Zhang, Yubing Qiu and Xingpeng Guo, *Corros. Sci.*, 74 (2013) 71.
22. X. Zhong, S. Yu, L. Chen, J. Hu and Z. Zhang, *J. Mater. Sci-Mater. El.*, 28 (2017) 2279.
23. B. Liao, Z. Chen, Y. Qiu and X. Guo, *Corros. Sci.*, 118 (2017) 190.
24. X. Zhong, G. Zhang and X. Guo, *Corros. Sci.*, 96 (2015) 1.
25. B. Liao, Z. Chen, Y. Qiu, G. Zhang and X. Guo, *Corros. Sci.*, 112 (2016) 393.
26. B. Liao, L. Wei, Z. Chen and X. Guo, *RSC Adv*, 7 (2017) 15060.
27. O. Devos, Gabrielli C, Beitone, L C.Mace and E.Ostermann H.Perrot, *J. Electroanal. Chem.*, 606 (2007) 85.
28. B. Medgyes, B. Illés and G. Harsányi, *J. Mater. Sci-Mater. El.*, 23(2012), 551.
29. X. Zhong, X. Guo, Y. Qiu, Z. Chen and G. Zhang, *J. Electrochem. Soc.*, 160 (2013) D495.
30. H. Ma, A. Kunwar, J. Chen, L. Qu, Y. Wang, X.G. Song, Peter Råback, H. Ma and N. Zhao, *Microelectron. Reliab.*, 83 (2018) 198.
31. L. Hua and H. N. Hou, *Microelectron. Reliab.*, 75 (2017) 27.
32. S. B. Lee, M. S. Jung , H. Y. Lee, T. Kang and Y. C Joo, *IEEE T Device Mat. Re.*, 9 (2009) 483.
33. B. Medgyes, B. Illés, R. Berényi and G. Harsányi, *J. Mater. Sci-Mater. El.*, 22 (2011) 694 .
34. B. Medgyes, B. Illés and G. Harsányi, *Periodica Polytechnica Electr Eng Co*, 57 (2013) 49.
35. X. Zhong, G. Zhang, Y. Qiu, Z. Chen, W. Zou and X. Guo, *Electrochem Commun.*, 27 (2013) 63.
36. X. He, M. H. Azarian and M. G. Pecht, *J. Electron. Mater.*, 40 (2011) 1921.